Cell. Mol. Life Sci. 64 (2007) 3139 – 3147
1420-682X/07/233139-9
DOI 10.1007/s00018-007-7268-7

Cellular and Molecular Life Sciences

Research Article

Wip1 protects hydrogen peroxide-induced colonic epithelial barrier dysfunction

T. Oshima[a,b,*], M. Sasaki[a], H. Kataoka[a], H. Miwa[b], T. Takeuchi[c] and T. Joh[a]

[a] Department of Internal Medicine and Bioregulation, Nagoya City University Graduate School of Medical Sciences, Kawasumi, Mizuho, Nagoya 467-8601 (Japan)
[b] Division of Upper Gastroenterology, Department of Internal Medicine, Hyogo College of Medicine, 1-1 Mukogawa, Nishinomiya, Hyogo 663-8501 (Japan), Fax: +81 798 45 6661, e-mail: t-oshima@hyo-med.ac.jp
[c] Department of Molecular Medicine, Institute for Molecular and Cellular Regulation, Gunma University, 3-39-15 Showa-machi, Maebashi 371-8512 (Japan)

Received 14 June 2007; received after revision 8 October 2007; accepted 8 October 2007
Online First 29 October 2007

Abstract. Tight junctions (TJs) create a paracellular permeability barrier. Although reactive oxygen species have been implicated as mediators of inflammation in inflammatory bowel diseases, their influence on the function of colonic epithelial TJs remains unknown. Oxidative stress-mediated colonic epithelial permeability was significantly attenuated by a p38 mitogen-activated protein (MAP) kinase inhibitor, SB203580. Although the amount of TJ proteins was not altered, hydrogen peroxide (H_2O_2) changed the localization of claudin-4 protein from an NP-40 insoluble fraction to a soluble fraction and from an apical TJ to lateral membrane. The p38 MAP kinase inactivator Wip1 significantly attenuated phosphorylation of p38 MAP kinase, and oxidative stress mediated permeability. H_2O_2-induced changes in claudin-4 localization were abolished by SB203580 pretreatment as well as Wip1-expressing adenovirus infection. This is the first study to demonstrate that exogenous Wip1 functions to protect oxidative stress-mediated colonic mucosal permeability and that H_2O_2-induced claudin-4 dislocalization is abolished by Wip1.

Keywords. Tight junction, Wip1, p38 MAP kinase, permeability, claudin-4.

Introduction

Throughout the gastrointestinal tract, a single layer of epithelial cells acts as a gateway that restricts uncontrolled entry of luminal antigens. This selective barrier function is critical for maintaining mucosal immune homeostasis. Intestinal epithelial barrier function is maintained by intracellular junctional complexes, including tight junctions (TJs), adherens junctions and desmosomes [1–4]. Of these, TJs are the most apical component of the intercellular junctional complexes [5]. The TJ separates the apical cell surface domains from the basolateral cell surface domains to establish cell polarity and also to provide a barrier, inhibiting solute and water flow through the paracellular space [6]. This selective barrier function is critical for maintaining mucosal immune homeostasis, as evidenced in colonic inflammation associated with the loss of epithelial integrity [7]. The TJs consist of occludin, the claudin family and JAM (junction adhesion molecule [8, 9].

* Corresponding author.

The claudins are a family of 24 distinct transmembrane proteins. They are composed of four transmembrane domains and two extracellular loops. Multiple claudin isoforms are expressed in a homophilic and heterophilic manner, and in varied patterns of tissue-specific expression [10] that regulate junctional permeability; the selectivity and strength of TJs are conferred to most cell types [11].

Hydrogen peroxide (H_2O_2), a colorless, highly toxic oxidizing agent, is constantly being generated within all cell types, including colonic epithelial cells, and must be quickly neutralized for the survival of cells [12, 13]. H_2O_2 is also reported to increase epithelial monolayer permeability by disrupting paracellular junctional complexes *in vitro* [14]. Grisham et al. reported a significant increase in mucosal permeability in acute inflammation of the bowel with H_2O_2 *in vivo* [15]. Epithelial resistance in ulcerative colitis (UC) is massively impaired, and the decreased barrier function is paralleled by a decrease in TJ strand count [2]. Altered epithelial permeability is also a consistent effect of H_2O_2 in other tissues, including renal cells [16].

Mitogen-activated protein (MAP) kinases, a family of serine-threonine kinases, have important roles as signal transducers. Hommes et al. demonstrated that guanylhydrazone, a c-Jun N-terminal kinase (JNK)/p38 inhibitor (CNI-1493), strongly reduces clinical disease activity in Crohn's disease patients [17]. Another study showed that an anti-inflammatory peptide, RDP58, which blocks pre-MAP kinase MyD88-IRAK-TRAF6 complex, is effective for the treatment of UC patients [18]. Activation of MAP kinases by various cytokines and growth factors is important in modulating cellular responses [19, 20], and the role of MAP kinase signaling has been of interest in TJ regulation [21, 22]. In addition, constitutive MAP kinase activation inhibits the formation of TJs in MDCK cells. Moreover, pharmacological inhibition of MAP kinase kinase (MEK) 1 signaling in these cells permits TJ formation [23]. The mitogenic effect of MAP kinase activity is logically opposed to TJ formation. We previously found that the MAP kinase and p38 MAP kinase pathways play an important role in H_2O_2-mediated disruption of endothelial TJs *in vitro* [24]. However, the detailed mechanisms, including the involvement of claudins, in the regulation of epithelial TJs during inflammation are as yet unclear. Signal transduction pathways, including MAP kinase and p38 MAP kinase, are involved in growth cell survival and cell death.

MAP kinase activation is often transient, and dephosphorylation by phosphatases plays a major role in the downregulation of MAP kinase activity under physiological conditions. Different phosphatases inactivate the MAP kinase cascades at different levels [25]. The protein phosphatase Wip1 was initially identified as a gene whose expression was induced by γ or UV (ultraviolet) radiation in a p53-dependent manner [26]. Wip1 is a nuclear protein [26] and a member of the serine/threonine-specific protein phosphatase type 2C (PP2C) family and is a potential downstream target of p53. *In vivo* and *in vitro* studies indicate that Wip1 selectively dephosphorylates and inactivates p38 MAP kinase, but not JNK, extracellular signal-regulated kinase (ERK) or MAP kinase kinases [25, 26]. Wip1 is induced by H_2O_2 in a p53-dependent manner. In order to study the exogenous Wip1 effect, we employed Caco-2 cells in which p53 is mutated.

In the present study, we examined the effect of H_2O_2 on colonic mucosal barrier properties and TJ organization and clarified which claudins are affected by H_2O_2. We also investigated the role of MAP kinases, using specific inhibitors and Wip1, a serine/threonine phosphatase against H_2O_2-induced increase in epithelial permeability.

Materials and Methods

Cell lines and culture conditions. Caco-2, a human colonic adenocarcinoma cell line, was obtained from American Type Culture Collection (Rockville, MD). Minimum Essential Medium Eagle (Sigma, St. Louis, MO, USA) was supplemented with 10 % FBS, 0.1 mM non-essential amino acids, 2.5 mg/ml amphotericin B, 50 U/ml penicillin and 50 mg/ml streptomycin. Culture medium was changed every 48–72 h.

Reagents and antibodies. Rabbit anti-claudin-1, rabbit anti-claudin-3 and mouse anti-claudin-4 antibodies were purchased from Zymed Laboratories (South San Francisco, CA, USA). Alexa 488-conjugated anti-mouse IgG (immunoglobulin G) antibody was obtained from Invitrogen (Carlsbad, CA, USA). Cy3-conjugated goat anti-rabbit IgG antibody was purchased from Jackson ImmunoResearch Laboratories (Westgrove, PA, USA). Anti-phospho-p38 MAP kinase antibody, an MEK inhibitor, PD98059, and a p38 MAP kinase inhibitor, SB203580, were obtained from Promega (Madison, WI, USA). Anti-p38 MAP kinase antibody was purchased from New England Biolabs (Beverly, MA, USA). All reagents were purchased from Sigma unless stated otherwise.

Construction of recombinant adenoviruses. Human FLAG-tagged Wip1 cDNA (complementary DNA) was inserted into the unique SwaI site of the full-length adenovirus genome cloned in the cassette cosmid, pAxCAwt (Takara Biomedical, Shiga,

Japan) to generate pAxCAwt-human Wip1. The resulting plasmid, which contains the Wip1 cDNA under the control of a CAG promoter (CMV enhancer, chicken β-actin promoter and part of an untranslated region of rabbit β-globin), was transfected into 293 cells. Recombinant Adv (Adv-Wip1) from a single plaque was expanded and purified twice by cesium chloride gradient ultracentrifugation. Viral titer was determined by plaque assay. Control Adv-lacZ, which carries β-gal cDNA, was isolated using the same procedure. Both recombinant viruses were dialyzed in PBS (pH 7.4), and stored in a solution of 10 % glycerol in PBS at −80°C until use. Adv-Wip1 and Adv-lacZ were infected into Caco-2 cells at a multiplicity of infection (MOI) of 10.

Wip1 expression was confirmed by detecting FLAG protein with anti-FLAG antibody by immunoblotting.

Trans-Epithelial Electrical resistance (TEER). Caco-2 cells were plated on 9-mm-diameter, 0.4-μm pore size tissue culture inserts (Becton Dickinson, Franklin Lakes, NJ, USA) at approximately 75 % confluency. The resistance across the monolayer was measured using MILLICELL-ERS (Millipore Corporation, Bedford, MA, USA) with 'chopstick' electrodes. The value obtained from a blank insert was subtracted to give the net resistance, which was multiplied by the membrane area to give the resistance in area-corrected units ($\Omega \cdot cm^2$). At 100 % confluence, trans-monolayer electrical resistance was measured.

The change in electrical resistance was represented by percentage baseline resistance, which was calculated as follows: % baseline resistance = [[resistance from each time point] – [resistance from a blank insert]]/[[baseline resistance] – [resistance from a blank insert]] × 100, where baseline resistance was the resistance at the 0 time point [27].

When resistance was stable (at $>280\ \Omega \cdot cm^2$), the culture medium from the upper (apical) compartment of the monolayer was removed and replaced with medium containing H_2O_2 (500 μM) or control medium. In some experiments, monolayers were pretreated with PD98059 (10 μM, 30 min), SB203580 (1 μM, 30 min) or Adv-Wip1 (10 MOI, 48 h) before addition of H_2O_2. Cell viability was assessed by measuring the release of lactate dehydrogenase (LDH) (LDH assay; Sigma) into the media. All data represent the average of four identically treated monolayers.

Western analysis of cell lysates. Western blot analysis was performed as previously described [28]. Cell lysates were prepared by adding 500 μl of boiling sample buffer [125 mM Tris/HCl (pH 6.8), 4 % SDS, 20 % glycerol, 10 % 2-mercaptoethanol, protease inhibitor cocktail and 0.025 % bromphenol blue] directly to a P60 culture dish.

For cell fractionation, cells were incubated in NP-40 lysis buffer (25 mM HEPES pH 7.4, 150 mM NaCl, 4 mM EDTA, 0.05 % NP-40, 1 mM Na_3VO_4, 25 mM NaF, protease inhibitor cocktail). The lysate was centrifuged at 600 × g for 10 min at 4 °C. The supernatant was transferred to another tube and centrifuged at 100 000 × g for 60 min at 4 °C. The supernatant was used as the NP-40 soluble fraction. The pellet was resuspended in 1 % SDS buffer (24 mM HEPES pH 7.5, 4 mM EDTA, 25 mM NaF, 1 mM Na_3VO_4, 1 % SDS, protease inhibitor cocktail), briefly sonicated on ice and then used as the NP-40 insoluble fraction. Protein concentrations were determined by the Bradford assay (Bio-Rad Laboratories, Hercules, CA, USA) according to the manufacturer's instructions.

Equal quantities of protein from each sample were electrophoretically separated on 7.5 % SDS-PAGE gels. Gels were transferred to nitrocellulose membranes (Amersham Life Science, Arlington Heights, IL, USA) and blocked with 5 % milk powder in PBS at 4 °C (overnight). The membrane was washed three times for 5 min each with wash buffer (0.1 % milk powder in PBS). The membrane was incubated with the appropriate primary antibody for 1 h at room temperature (RT). The membrane was washed in 0.1 % milk/PBS three times for 5 min each with wash buffer and then incubated with the appropriate secondary horseradish peroxidase-conjugated anti-rabbit or mouse IgG antibody for 1 h at RT. Lastly, the membrane was washed three times and developed using the enhanced chemiluminescence (ECL) detection system (Amersham, La Jolla, CA, USA). All experiments were reproduced three times, the results of a typical experiment are shown.

Real-time PCR. For real-time quantitative reverse-transcription PCR, total RNA was prepared from control and treated Caco-2 cells using the RNeasy mini kit (Qiagen, Valencia, CA, USA). cDNA was prepared using the cDNA synthesis kit (Perkin-Elmer Applied Biosystems, Foster City, CA, USA) with random hexamers using 1 μg of total RNA [29, 30]. The level of mRNA (messenger RNA) expression of Wip1 was analyzed by real-time PCR using the ABI Prism 7700 Sequence Detection System (Applied Biosystems). A TaqMan probe and primer set designed to amplify the Wip1 gene construct was used to quantitate 5 μl of cell lysate in a total PCR volume of 50 μl. Reagents utilized included the TaqMan 2× Universal Master Mix containing 1× TaqMan buffer A, 5 mM $MgCl_2$, 400 μM dUTP, 200 μM dATP, dCTP, dGTP, 8 % glycerol, AmpliTaq Gold (0.025 U/μl),

AmpErase UNG (0.01 U/μl), 300 nM of each forward and reverse primer, and a 100 nM probe. The kit was utilized according to the manufacturer's instructions. The PCR cycling conditions for all samples were as follows: 50 °C, 2 min for AmpErase UNG incubation, 95 °C, 10 min for AmpliTaq Gold activation and 40 cycles for the melting (95 °C, 15 s) and annealing/extension (60 °C for 1 min) steps. PCR reactions for each template were performed in duplicate in 96-well plates. Significant contamination with genomic DNA was excluded by amplifying non-reverse-transcribed RNA. Data analysis was performed with the ABI PRISM sequence detection software. The relative expression of each mRNA was calculated by the ΔCt method (where ΔCt is the value obtained by subtracting the ΔCt value for GAPDH mRNA from the Ct value for the target mRNA) (Applied Biosystems), as employed in previous studies [31, 32].

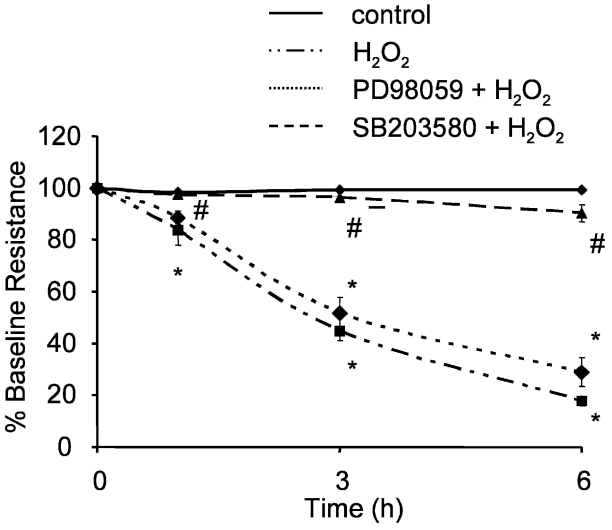

Figure 1. Effects of MEK and p38 MAP kinase inhibitors on the H_2O_2-induced reduction in electrical resistance of a Caco-2 cell monolayer. H_2O_2 (500 μM) treatment of colonic epithelial monolayers caused a significant decrease in TEER at 3 and 6 h after stimulation. Although an MEK inhibitor, PD98059 (10 μM), did not have any effect, a p38 MAP kinase inhibitor, SB203580 (1 μM), significantly inhibited the H_2O_2-induced decrease in electrical resistance. Control: untreated control. *, $P < 0.05$ vs. baseline; #, $P < 0.05$ vs. H_2O_2.

Epithelial permeability. We also measured epithelial permeability in response to H_2O_2 exposure using fluorescein isothiocyanate labeled dextran (FITC-dextran) (MW 4000) as a permeable tracer that will pass across the epithelial monolayer using the method described by Maruo et al. [33] with minor modifications [34]. Caco-2 cells were grown on the surface of 0.4-μm pore size tissue culture inserts (Becton Dickinson). These cell monolayers were washed twice with Hank's balanced salt solution (HBSS), and then placed on 24-well plates with 1 ml of HBSS in the lower chamber. Five hundred microliters of HBSS containing 5 mg/ml of FITC-dextran were put into the luminal chamber, and then the apparatus was placed in a CO_2 incubator at 37 °C. After incubation for 30 min, a 100-μl sample was taken from the lower chamber and the absorbance of FITC-dextran was determined at 492 nm with a spectrophotometer (Fluoroskan Ascent). The data were expressed as follows: FITC-dextran permeability index (%) = [[experimental clearance] – [spontaneous clearance]]/[[clearance of filter alone] – [spontaneous clearance]] × 100.

Permeability measurements were made under control conditions, following exposure to H_2O_2 (500 μM) and following pretreatment with SB203580 (1 μM, 30 min) or Adv-Wip1 (10 MOI, 48 h). After the pretreatment, H_2O_2 was added to the culture, and permeability measured at 6 h after stimulation.

Immunofluorescence staining of junctional proteins. Caco-2 cells were seeded onto 1.2-cm-diameter coverslips and allowed to reach confluency. Monolayers were exposed to H_2O_2 with and without Adv-Wip1 infection or appropriate buffer controls. Samples were fixed with ethanol (30 min) and acetone (1 min) [35] and stained for claudins. Primary rabbit anti-claudin-3 polyclonal antibody and/or mouse anti-claudin-4 monoclonal antibody were used at a concentration of 4 μg/ml. Cy3-conjugated goat anti-rabbit IgG and Alexa488 anti-mouse IgG secondary antibodies were used at a 1 : 200 dilution. The specificity of the reaction was tested by incubation with HBSS, non-immune rabbit serum or mouse IgG1. Slides were viewed using a confocal laser scanning microscope. Pictures were recorded on a Windows computer using a 40× objective.

Statistical analysis. All data are expressed as mean ± SE. Data were analyzed using one-way ANOVA (analysis of variances) with Bonferroni's correction for multiple comparisons. Significance was accepted at $P < 0.05$.

Results

Effect of H_2O_2 on TEER of Caco-2 monolayer. H_2O_2 (500 μM) treatment of colonic epithelial monolayers caused a significant decrease in TEER at 3 and 6 h after stimulation (Fig. 1). There was no evidence of cytotoxic effects with H_2O_2 solution at any time point, as determined by the LDH (lactate dehydrogenase) release assay (data not shown). Although pretreatment with the MEK inhibitor PD98059 (10 μM) did

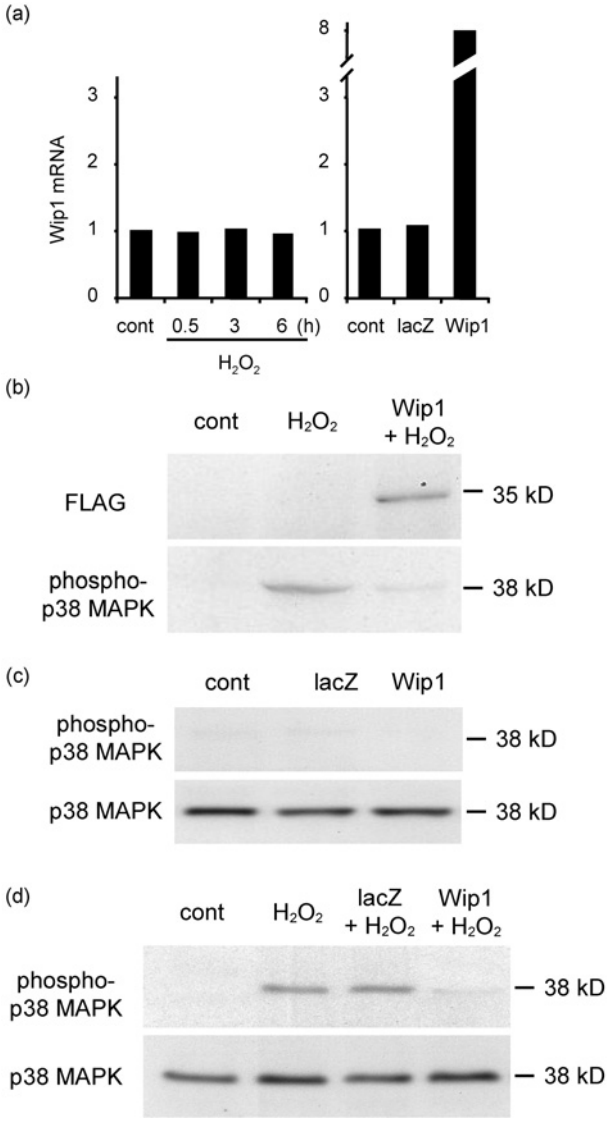

Figure 2. Infection with Adv-Wip1. (*a*) Wip1 mRNA was induced by Adv-Wip1 (Wip1) infection but not by H_2O_2 (500 μM) stimulation or Adv-lacZ (lac Z) infection. (*b*) FLAG-tagged Wip1 expression was induced by the infection. H_2O_2-induced phosphorylation of p38 MAP kinase (phospho-p38 MAPK) was attenuated by Adv-Wip1 infection. (*c*) Adv-lacZ (lac Z) or Adv-Wip1 (Wip1) did not induce p38 MAP kinase phosphorylation. (*d*) Adv-lacZ (lac Z) did not affect the H_2O_2-induced phosphorylation of p38 MAP kinase. Cont: untreated control.

not have any effect on the H_2O_2-induced decrease in TEER, pretreatment with the p38 MAP kinase inhibitor SB203580 (1 μM) significantly inhibited the H_2O_2-induced decrease in TEER. Pretreatment of monolayers with PD98059 and SB203580 did not influence the TEER at baseline.

Establishment of Wip1-expressing adenovirus. Wip1-expressing adenovirus was established as described in 'Materials and methods'. Infection of the virus in Caco-2 cells was confirmed by real-time PCR and Western blotting. Wip1 mRNA was induced by Adv-Wip1 infection, but not by H_2O_2 (500 μM) stimulation or by Adv-lacZ infection (Fig. 2a). Although Wip1 is reported to be induced in H_2O_2 [26], Wip1 is induced by a p53-dependent manner [25] and p53 is mutated in Caco-2 cells. Induction of FLAG protein was confirmed using anti-FLAG antibody. H_2O_2 (500 μM, 1 h) induced the phosphorylation of p38 MAP kinase, and Adv-Wip1 infection (10 MOI, 48 h) attenuated phosphorylation of p38 MAP kinase (Fig. 2b). Adv-lacZ or Adv-Wip1 infection did not induce phosphorylation of p38 MAP kinase (Fig. 2c). Adv-lacZ infection did not affect the H_2O_2-induced phosphorylation of p38 MAP kinase (Fig. 2d).

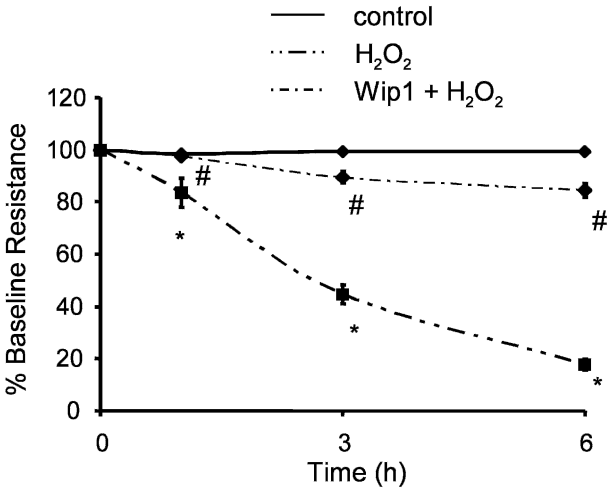

Figure 3. Effect of Wip1 on the H_2O_2-induced reduction in electrical resistance of a Caco-2 monolayer. Wip1-expressing adenovirus infection significantly inhibited the H_2O_2-induced decrease in electrical resistance. Control: untreated control. *, $P < 0.05$ vs. baseline; #, $P < 0.05$ vs. H_2O_2.

Effect of Wip1 on colonic epithelial permeability. Adv-Wip1 infection significantly blocked the H_2O_2-induced decrease in electrical resistance (Fig. 3). Adv-Wip1 infection itself did not influence the TEER (data not shown). Paracellular permeability of Caco-2 cells was also measured using FITC-dextran (MW 4000). The amount of FITC-dextran that passed across an epithelial monolayer was measured with a plate spectrophotometer. H_2O_2 (500 μM, 6 h) significantly increased FITC-dextran permeability (Fig. 4). These data suggest that H_2O_2 induced a break in the mucosal barrier of Caco-2 cells. P38 MAPK inhibitor, SB203580 and Adv-Wip1 infection significantly attenuated the H_2O_2-induced increase in FITC-dextran permeability. These data are consistent with the data of TEER.

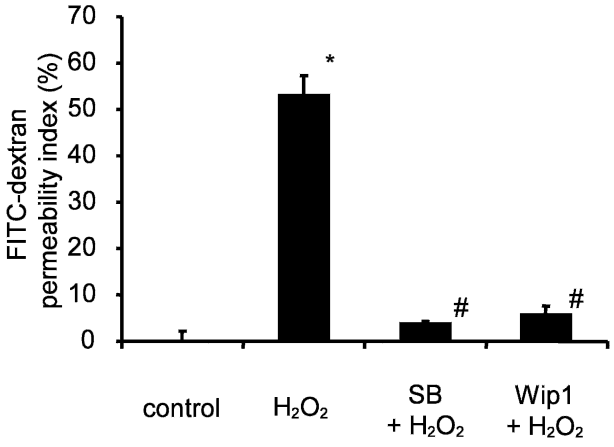

Figure 4. Effects of a p38 MAP kinase inhibitor and Wip1 infection on H_2O_2-induced FITC-dextran permeability. H_2O_2 (500 μM, 6 h) significantly increased FITC-dextran permeability. SB203580 (SB) and Adv-Wip1 significantly blocked H_2O_2-induced FITC-dextran permeability. (n = 5). Control: untreated control. *, $P < 0.05$ vs. untreated control. #, $P < 0.05$ vs. H_2O_2.

H_2O_2 induces translocation of claudin-4 from TJ. There were no changes in the levels of these claudin-1, claudin-3 and claudin-4 proteins in total cell extract after stimulation with H_2O_2 (500 μM, 6 h) (Fig. 5). Claudin-1 and claudin-3 solubility in NP-40 were unchanged after stimulation with H_2O_2, while claudin-4 solubility did change after stimulation with H_2O_2; claudin-4 moved from the NP-40-insoluble fraction to the NP-40-soluble fraction, suggesting that claudin-4 was no longer in the TJs. Claudin-3 was not affected by the p38 MAP kinase inhibitor SB203580. On the other hand, claudin-4 solubility relocated from the NP-40 soluble to the NP-40-insoluble fraction upon SB203580 pretreatment. This finding may be related to impaired barrier function in H_2O_2-treated Caco-2 cells. Adv-Wip1 infection did not change claudin-3 expression or NP-40 solubility of claudin-3. Although claudin-4 expression was not changed in total by Adv-Wip1 infection, Adv-Wip1 infection attenuated the H_2O_2-induced change in the NP-40 solubility of claudin-4.

Claudin-3 and claudin-4 were expressed at junctions under control conditions, as determined by immunofluorescence staining (Fig. 6). H_2O_2 stimulation changed the localization of claudin-4, which was expressed at the lateral membrane but more broadly than claudin-3, as indicated in the xz projection by confocal microscopy. This suggests that claudin-4 moved from the TJ to the subjunctional lateral membrane. H_2O_2-induced changes in claudin-4 localization were abolished by SB203580 pretreatment (data not shown) and Adv-Wip1 pretreatment. Claudin-3 expression was not affected by H_2O_2 stimulation or Adv-Wip1 infection.

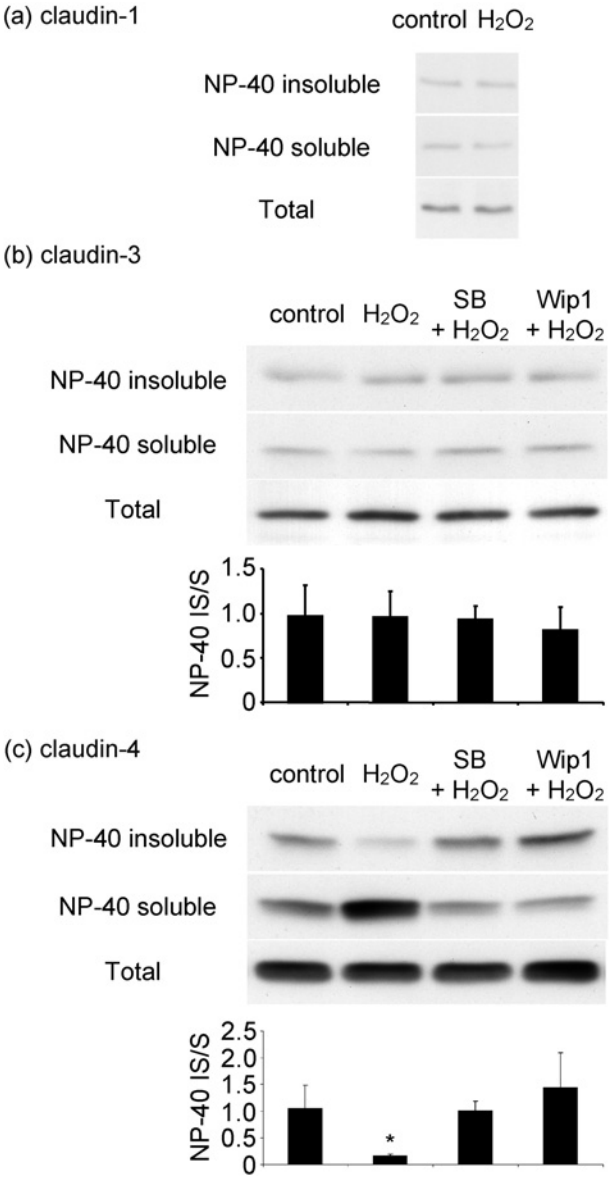

Figure 5. Change in solubility of claudin-4 after H_2O_2 stimulation. H_2O_2 did not change the total amount of claudin-1, claudin-3 or claudin-4 proteins, as determined by Western blotting (*a–c*). Claudin-1 and claudin-3 NP-40 solubility was not changed after stimulation with H_2O_2 (*a*, *b*). On the other hand, claudin-4 NP-40 solubility was significantly changed on stimulation with H_2O_2 (*c*). Claudin-4 has moved from the NP-40 insoluble fraction to the NP-40 soluble fraction. Claudin-3 was not affected by pretreatment with SB203580 (SB) or pretreatment with Adv-Wip1. On the other hand, claudin-4 solubility returned from the NP-40-soluble to the NP-40-insoluble fraction with SB203580 or Adv-Wip1 pretreatment. (n = 3). *, $P < 0.05$ vs. untreated control, SB + H_2O_2 and Wip1 + H_2O_2.

Discussion

Intestinal epithelial cell layers play a critical role by separating physiologically distinct compartments and protect against uncontrolled entry of luminal antigens. The importance of maintaining the integrity of TJs is

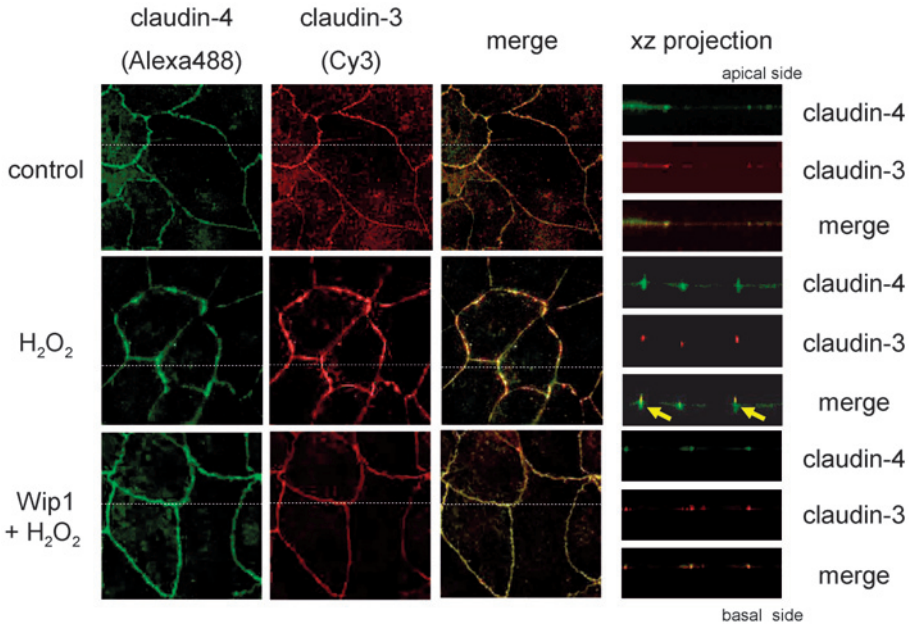

Figure 6. Immunofluorescent staining of claudin-3 and claudin-4. Claudin-3 and claudin-4 were expressed at junctions under control conditions. Both claudin-3 and claudin-4 were co-localized at the junctions. H_2O_2-stimulation changed the localization of claudin-4, with claudin-4 being expressed at the lateral membrane more broadly than claudin-3 (arrows), when the *xz* projection was checked by confocal microscopy. Pretreatment of Adv-Wip1 abolished the H_2O_2-induced change in claudin-4 localization. Claudin-3 expression was not affected by H_2O_2 stimulation or by Adv-Wip1 pretreatment. Control: untreated control. The position of the z-scan is indicated by the dotted lines.

underscored by recent reports indicating that increased intestinal permeability contributes to the pathogenesis of several intestinal disorders, including inflammatory bowel disease (IBD) [2, 36]. Thus, our aims were to define the mechanism behind oxidative stress-induced barrier dysfunction and to determine whether blockade of MAP kinases could prevent epithelial barrier dysfunction induced by oxidative stress. In the present study we have demonstrated that pharmacological inhibition of p38 signaling in H_2O_2 stimulated Caco-2 cells functionally protects the barrier function. Concerning the Caco-2 cell condition, although a previous report indicated that H_2O_2-stimulation at 150 μM for 30 min increased LDH activity in Caco-2 cells [37], LDH activity was not increased with H_2O_2 (500 μM) in our study. Furthermore, H_2O_2-induced decrease in TEER and H_2O_2-induced increase in FITC-dextran permeability were reversed by SB203580 pretreatment or Wip1 infection. It may be because of the cell conditions. However, we cannot explain the discrepancy precisely at this time.

The loss of TJ barrier function by deleterious inflammatory mechanisms is an important concept in colonic physiology. The TJs of epithelial cells from different origins are affected by H_2O_2, and enhanced protein tyrosine phosphorylation is a contributory factor for the enhanced permeability of epithelial cells [38]. Although several studies indicate that MEK1 signaling increases paracellular permeability [39], there exists some disparity in observed cellular responses. Recently, a report demonstrated that inhibition of MEK1 signaling did not influence expression of occludin or claudin-1 and did not affect TJ function in breast cancer cells [40]. Another study using *Escherichia coli* showed that ERK1/2 was activated in T84 cells, but did not induce TJ barrier disruptions as measured by TEER [41]. Recent studies suggest that TJs are regulated in some tissues *in vitro* and *in vivo* through the p38 MAP kinase signaling pathway [24, 42, 43]. TGF(transforming growth factor)-β3 regulates the blood-testis barrier *in vivo* and *in vitro* via the p38 MAP kinase pathway [42]. Yamamoto et al. reported that expression and function of TJs during regeneration of rat hepatocytes are partly controlled via the p38 MAP kinase signaling pathway [43]. Thus, the roles of MAP kinases in epithelial barrier function and TJs are numerous and may depend on cell type or stimulant specificity.

p38 MAP kinase inhibitors are efficacious in several disease models, including inflammation, arthritis and other joint diseases, septic shock and myocardial injury [44]. Furthermore, there is progress towards clinical development of p38 MAP kinase inhibitors for the treatment of inflammatory diseases [45]. For example, CNI-1493 MAP kinase inhibitor is effective in the treatment of Crohn's disease [17], and an anti-inflammatory peptide, RDP58, which blocks pre-MAP kinase MyD88-IRAK-TRAF6 complex, is effective in the treatment of UC [18]. Considering the treatment of inflammatory diseases by blocking the activation of p38 MAP kinase, SB203580 is a chemical inhibitor and may be toxic. Wip1 has been reported to dephosphorylate and to inactivate p38 but not JNK or ERK [25]. Our results suggest that Wip1 exists even in physiological condition and that exogenous Wip1 can

prevent the oxidative stress-induced activation of p38 MAP kinase. Although Wip1 expression is induced in a p53-dependent manner [26] and is induced by H_2O_2 [25], p53 is mutated in Caco-2 cells. Therefore, using Caco-2 cells in this study was useful for understanding the effects of exogenous Wip1 under H_2O_2 stimulation. Exogenous Wip1 treatment or endogenous Wip1 production is suggested to prevent oxidative stress-induced p38 MAP kinase activation followed by the disruption of TJs.

Claudins are important for TJ formation, and epithelial barrier disruption is induced by claudin-4 removal from TJs [46, 47]. The barrier role of claudin-4 has also been suggested by an overexpression study, in which overexpression of claudin-4 increased TEER and the number of junctional strands [48]. These data are consistent with our result showing H_2O_2-induced change in claudin-4 localization and colonic epithelial permeability. Detergent insolubility of proteins is considered to indicate their integration into macromolecular complexes such as intercellular junctions. The heterogeneous response of TJ proteins to H_2O_2 may be due to junctional remodeling, which may involve additional protein synthesis and altered turnover rates.

Loss of claudin-2 expression from Madin-Darby canine kidney (MDCK) cells by siRNA (small interfering RNA) dramatically increased TEER. In contrast, loss of claudin-4 or claudin-7 expression significantly decreased TEER [49]. Claudin-1 and claudin-3 siRNA did not change the TEER even when the expression of each protein was blocked. In this study we did not show directly that H_2O_2-induced increase in epithelial permeability was mediated by claudin-4. It is possible that other TJ protein expression changes such as a decrease of claudin-7 or an increase of claudin-2 may be involved in H_2O_2-induced increase in epithelial permeability. To precisely define the TJ proteins which modulate epithelia permeability following H_2O_2 exposure clearly requires further investigation.

To our knowledge this is the first report demonstrating that H_2O_2 increases colonic permeability via the activation of p38 MAP kinase and that H_2O_2-induced increase in colonic permeability is abolished by the p38 MAP kinase-specific phosphatase Wip1. H_2O_2-induced change in claudin-4 localization is also abolished by Wip1. Further studies are required to evaluate the effect of Wip1 *in vivo*. Maintaining the function of TJs by Wip1 is a potentially new therapeutic approach in the treatment of IBDs.

Acknowledgments. We thank Yukimi Itoh for her expert tissue culture and technical assistance. This study was supported by the Ministry of Education, Culture, Sports, Science and Technology of Japan through a Grant-in-Aid for Young Scientists (B) 2005–2006 (no. 17790459), and by a grant from Hyogo College of Medicine.

1 Jankowski, J. A., Bedford, F. K., Boulton, R. A., Cruickshank, N., Hall, C., Elder, J., Allan, R., Forbes, A., Kim, Y. S., Wright, N. A. et al. (1998) Alterations in classical cadherins associated with progression in ulcerative and Crohn's colitis. Lab. Invest. 78, 1155–1167.
2 Schmitz, H., Barmeyer, C., Fromm, M., Runkel, N., Foss, H. D., Bentzel, C. J., Riecken, E. O. and Schulzke, J. D. (1999) Altered tight junction structure contributes to the impaired epithelial barrier function in ulcerative colitis. Gastroenterology 116, 301–309.
3 Kinugasa, T., Sakaguchi, T., Gu, X. and Reinecker, H. C. (2000) Claudins regulate the intestinal barrier in response to immune mediators. Gastroenterology 118, 1001–1011.
4 North, A. J., Bardsley, W. G., Hyam, J., Bornslaeger, E. A., Cordingley, H. C., Trinnaman, B., Hatzfeld, M., Green, K. J., Magee, A. I. and Garrod, D. R. (1999) Molecular map of the desmosomal plaque. J. Cell Sci. 112 (Pt 23), 4325–4336.
5 Farquhar, M. G. and Palade, G. E. (1963) Junctional complexes in various epithelia. J. Cell Biol. 17, 375–412.
6 Tsukita, S. and Furuse, M. (2000) Pores in the wall: claudins constitute tight junction strands containing aqueous pores. J. Cell Biol. 149, 13–16.
7 Hermiston, M. L. and Gordon, J. I. (1995) Inflammatory bowel disease and adenomas in mice expressing a dominant negative N-cadherin. Science 270, 1203–1207.
8 Gumbiner, B. M. (1993) Breaking through the tight junction barrier. J. Cell Biol. 123, 1631–1633.
9 Tsukita, S., Furuse, M. and Itoh, M. (2001) Multifunctional strands in tight junctions. Nat. Rev. Mol. Cell Biol. 2, 285–293.
10 Hewitt, K. J., Agarwal, R. and Morin, P. J. (2006) The claudin gene family: expression in normal and neoplastic tissues. BMC Cancer 6, 186.
11 Morin, P. J. (2005) Claudin proteins in human cancer: promising new targets for diagnosis and therapy. Cancer Res. 65, 9603–9606.
12 Parks, D. A. (1989) Oxygen radicals: mediators of gastrointestinal pathophysiology. Gut 30, 293–298.
13 Thannickal, V. J. and Fanburg, B. L. (2000) Reactive oxygen species in cell signaling. Am. J. Physiol. Lung Cell. Mol. Physiol. 279, L1005–L1028.
14 Rao, R. K., Baker, R. D., Baker, S. S., Gupta, A. and Holycross, M. (1997) Oxidant-induced disruption of intestinal epithelial barrier function: role of protein tyrosine phosphorylation. Am. J. Physiol. 273, G812–G823.
15 Grisham, M. B., Gaginella, T. S., von Ritter, C., Tamai, H., Be, R. M. and Granger, D. N. (1990) Effects of neutrophil-derived oxidants on intestinal permeability, electrolyte transport, and epithelial cell viability. Inflammation 14, 531–542.
16 Meyer, T. N., Schwesinger, C., Ye, J., Denker, B. M. and Nigam, S. K. (2001) Reassembly of the tight junction after oxidative stress depends on tyrosine kinase activity. J. Biol. Chem. 276, 22048–22055.
17 Hommes, D., van den Blink, B., Plasse, T., Bartelsman, J., Xu, C., Macpherson, B., Tytgat, G., Peppelenbosch, M. and Van Deventer, S. (2002) Inhibition of stress-activated MAP kinases induces clinical improvement in moderate to severe Crohn's disease. Gastroenterology 122, 7–14.
18 Travis, S., Yap, L. M., Hawkey, C., Warren, B., Lazarov, M., Fong, T. and Tesi, R. J. (2005) RDP58 is a novel and potentially effective oral therapy for ulcerative colitis. Inflamm. Bowel Dis. 11, 713–719.
19 Hagemann, C. and Blank, J. L. (2001) The ups and downs of MEK kinase interactions. Cell Signal. 13, 863–875.
20 Bogoyevitch, M. A. and Court, N. W. (2004) Counting on mitogen-activated protein kinases – ERKs 3, 4, 5, 6, 7 and 8. Cell. Signal. 16, 1345–1354.

21 Schneeberger, E. E. and Lynch, R. D. (2004) The tight junction: a multifunctional complex. Am. J. Physiol Cell Physiol 286, C1213–C1228.
22 Matter, K. and Balda, M. S. (2003) Signalling to and from tight junctions. Nat. Rev. Mol .Cell Biol. 4, 225–236.
23 Chen, Y., Lu, Q., Schneeberger, E. E. and Goodenough, D. A. (2000) Restoration of tight junction structure and barrier function by down-regulation of the mitogen-activated protein kinase pathway in ras-transformed Madin-Darby canine kidney cells. Mol. Biol. Cell 11, 849–862.
24 Kevil, C. G., Oshima, T. and Alexander, J. S. (2001) The role of p38 MAP kinase in hydrogen peroxide mediated endothelial solute permeability. Endothelium 8, 107–116.
25 Takekawa, M., Adachi, M., Nakahata, A., Nakayama, I., Itoh, F., Tsukuda, H., Taya, Y. and Imai, K. (2000) p53-inducible wip1 phosphatase mediates a negative feedback regulation of p38 MAPK-p53 signaling in response to UV radiation. EMBO J. 19, 6517–6526.
26 Fiscella, M., Zhang, H., Fan, S., Sakaguchi, K., Shen, S., Mercer, W. E., Vande Woude, G. F., O'Connor, P. M. and Appella, E. (1997) Wip1, a novel human protein phosphatase that is induced in response to ionizing radiation in a p53-dependent manner. Proc. Natl. Acad. Sci. USA 94, 6048–6053.
27 Oshima, T., Laroux, F. S., Coe, L. L., Morise, Z., Kawachi, S., Bauer, P., Grisham, M. B., Specian, R. D., Carter, P., Jennings, S. et al. (2001) Interferon-gamma and interleukin-10 reciprocally regulate endothelial junction integrity and barrier function. Microvasc. Res. 61, 130–143.
28 Oshima, T., Pavlick, K. P., Laroux, F. S., Verma, S. K., Jordan, P., Grisham, M. B., Williams, L. and Alexander, J. S. (2001) Regulation and distribution of MAdCAM-1 in endothelial cells in vitro. Am. J. Physiol. Cell Physiol. 281, C1096–1105.
29 Heid, C. A., Stevens, J., Livak, K. J. and Williams, P. M. (1996) Real time quantitative PCR. Genome Res. 6, 986–994.
30 Gibson, U. E., Heid, C. A. and Williams, P. M. (1996) A novel method for real time quantitative RT-PCR. Genome Res. 6, 995–1001.
31 Nishimura, M., Imai, T., Morioka, Y., Kuribayashi, S., Kamataki, T. and Naito, S. (2004) Effects of NO-1886 (Ibrolipim), a lipoprotein lipase-promoting agent, on gene induction of cytochrome P450 s, carboxylesterases, and sulfotransferases in primary cultures of human hepatocytes. Drug Metab. Pharmacokinet. 19, 422–429.
32 Nishimura, M., Naito, S. and Yokoi, T. (2004) Tissue-specific mRNA expression profiles of human nuclear receptor subfamilies. Drug Metab. Pharmacokinet. 19, 135–149.
33 Maruo, N., Morita, I., Shirao, M. and Murota, S. (1992) IL-6 increases endothelial permeability in vitro. Endocrinology 131, 710–714.
34 Oshima, T., Flores, S. C., Vaitaitis, G., Coe, L. L., Joh, T., Park, J. H., Zhu, Y., Alexander, B. and Alexander, J. S. (2000) HIV-1 Tat increases endothelial solute permeability through tyrosine kinase and mitogen-activated protein kinase-dependent pathways. AIDS 14, 475–482.
35 Oshima, T., Blaschuk, O., Gour, B., Symonds, M., Elrod, J. W., Sasaki, M., Jackson, T. H. and Alexander, J. S. (2003) Tight junction peptide antagonists enhance neutrophil trans-endothelial chemotaxis. Life Sci. 73, 1729–1740.
36 Farhadi, A., Banan, A., Fields, J. and Keshavarzian, A. (2003) Intestinal barrier: an interface between health and disease. J. Gastroenterol. Hepatol. 18, 479–497.
37 Wijeratne, S. S., Cuppett, S. L. and Schlegel, V. (2005) Hydrogen peroxide induced oxidative stress damage and antioxidant enzyme response in Caco-2 human colon cells. J. Agric. Food Chem. 53, 8768–8774.
38 Jepson, M. A. (2003) Disruption of epithelial barrier function by H2O2: distinct responses of Caco-2 and Madin-Darby canine kidney (MDCK) strains. Cell. Mol. Biol. (Noisy-le-grand) 49, 101–112.
39 Kevil, C. G., Oshima, T., Alexander, B., Coe, L. L. and Alexander, J. S. (2000) H(2)O(2)-mediated permeability: role of MAPK and occludin. Am. J. Physiol. Cell. Physiol. 279, C21–C30.
40 Macek, R., Swisshelm, K. and Kubbies, M. (2003) Expression and function of tight junction associated molecules in human breast tumor cells is not affected by the Ras-MEK1 pathway. Cell. Mol. Bio.l (Noisy-le-grand) 49, 1–11.
41 Savkovic, S. D., Ramaswamy, A., Koutsouris, A. and Hecht, G. (2001) EPEC-activated ERK1/2 participate in inflammatory response but not tight junction barrier disruption. Am. J. Physiol. Gastrointest. Liver Physiol. 281, G890–G898.
42 Lui, W. Y., Lee, W. M. and Cheng, C. Y. (2003) TGF-betas: their role in testicular function and Sertoli cell tight junction dynamics. Int. J. Androl. 26, 147–160.
43 Yamamoto, T., Kojima, T., Murata, M., Takano, K., Go, M., Hatakeyama, N., Chiba, H. and Sawada, N. (2005) p38 MAP-kinase regulates function of gap and tight junctions during regeneration of rat hepatocytes. J. Hepatol. 42, 707–718.
44 Lee, J. C., Kassis, S., Kumar, S., Badger, A. and Adams, J. L. (1999) p38 mitogen-activated protein kinase inhibitors – mechanisms and therapeutic potentials. Pharmacol. Ther. 82, 389–397.
45 Kumar, S., Boehm, J. and Lee, J. C. (2003) p38 MAP kinases: key signalling molecules as therapeutic targets for inflammatory diseases. Nat. Rev. Drug Discov. 2, 717–726.
46 Furuse, M., Fujita, K., Hiiragi, T., Fujimoto, K. and Tsukita, S. (1998) Claudin-1 and -2: novel integral membrane proteins localizing at tight junctions with no sequence similarity to occludin. J. Cell Biol. 141, 1539–1550.
47 Sonoda, N., Furuse, M., Sasaki, H., Yonemura, S., Katahira, J., Horiguchi, Y. and Tsukita, S. (1999) Clostridium perfringens enterotoxin fragment removes specific claudins from tight junction strands: Evidence for direct involvement of claudins in tight junction barrier. J. Cell Biol. 147, 195–204.
48 Van Itallie, C., Rahner, C. and Anderson, J. M. (2001) Regulated expression of claudin-4 decreases paracellular conductance through a selective decrease in sodium permeability. J. Clin. Invest. 107, 1319–1327.
49 Hou, J., Gomes, A. S., Paul, D. L. and Goodenough, D. A. (2006) Study of claudin function by RNA interference. J. Biol. Chem. 281, 36117–36123.